TEKA. COMMISSION OF MOTORIZATION AND ENERGETICS IN AGRICULTURE – 2012, Vol. 12, No. 2, 203–208

An algorithm for identification of the relaxation spectrum of viscoelastic materials from discrete-time stress relaxation noise data

Anna Stankiewicz

Department of Mechanical Engineering and Automatics
University of Life Sciences in Lublin
Doświadczalna 50A, 20-280 Lublin, Poland
e-mail: anna.stankiewicz@up.lublin.pl

Summary. New algorithm of the least-squares approximation of the spectrum of relaxation frequencies by the finite series of Hermite functions using discrete-time noise corrupted measurements of relaxation modulus obtained in stress relaxation test has been proposed. Since the problem of relaxation spectrum identification is ill-posed, the inverse problem of Tikhonov regularization with guaranteed model approximation is used to achieve the stability of the scheme. The linear convergence of approximations generated by the scheme is proved for noise measurements. It is also indicated that the accuracy of the spectrum approximation depends both on measurement noises and regularization parameter and on the proper selection of time-scale parameter of the basis functions. The validity and effectiveness of the method is demonstrated using simulated data of Gaussian relaxation spectrum. Applying the proposed scheme, the relaxation spectrum of an unconfined cylindrical specimen of the beet sugar root is determined.

Key words: relaxation spectrum, identification algorithm, regularization, Hermite functions

INTRODUCTION

The selection of an appropriate mathematical representation is of central importance in the analysis of a physical system. Essentially, the choice of respective model depends on two criteria: the particular characteristics to be abstracted and our ability to specify the representation quantitatively. System identification deals with the problem of building mathematical models of systems (processes) based on observed data. In order to find such a model, which will describe well the system (process), an appropriate identification method must be derived [16].

In rheology it is assumed that the relaxation modulus $G(t)$ has the following representation [5,18]:

$$G(t)=\int_0^\infty H(\nu)\,e^{-t\nu}d\nu, \tag{1}$$

where: $H(\nu)$ His the spectrum of relaxation frequencies $\nu\geq 0$.

Since, as it is well-known, for many materials the long-term modulus $lim_{t\to\infty}\, G(t)=G_\infty>0$ (see [18,21], as well as the Example 3 below), instead of the classical equation (1), it is convenient to consider the following 'more-realistic' augmented material description:

$$\bar{G}(t)=\int_0^\infty H(\nu)e^{-t\nu}d\nu+G_\infty=G(t)+G_\infty. \tag{2}$$

The spectrum is recovered from discrete-time measurements $\bar{G}(t_i)=G(t_i)+z(t_i)$, $i=1,\ldots,N$, of relaxation modulus obtained in stress relaxation test. Here $z(t_i)$ is additive measurement noise. A complication for determining the relaxation spectrum is, that this problem is undetermined and ill-conditioned in the Hadamard sense [11,21]. Due to the noise or truncation of the experimental data, many models may fit the relaxation modulus experimental data adequately, but small errors in the data may lead to large changes in the determined models. The mathematical difficulties can be overcome by synthesis of an appropriate identification algorithm. In the paper [22] the following model of the spectrum $H(\nu)$ is taken:

$$H_K(\nu)=\sum_{k=0}^{K-1} g_k\,h_k(\nu), \tag{3}$$

where: g_k are constants and $h_k(\nu)$ are Hermite functions:

$$h_k(\nu)=\frac{\sqrt{\alpha}}{\sqrt{2^k\,k!}\sqrt[4]{\pi}}e^{-(\alpha\nu)^2/2}\,P_k(\alpha\nu),\quad k=0,1,\ldots, \tag{4}$$

with: Hermite polynomial $P_k(x)$ defined by [22; eqs. (3), (4)]. Here notation [22; eqs. (3), (4)] is used for the

equations (3) and (4) in the paper [22]. The square index [12,14,16] is applied:

$$Q_N\left(\boldsymbol{g}_K\right)=\sum_{i=1}^{N}\left[\overline{G}\left(t_i\right)-\overline{G}_K\left(t_i\right)\right]^2, \tag{5}$$

and the resulting task of the least-squares approximation of the spectrum $H(\nu)$ by the linear combination of Hermite functions is solved. Tikhonov regularization [24] is used to guarantee the stability of the scheme for computing the vector $\boldsymbol{g}_K=\left[g_0 \quad \ldots \quad g_{K-1} \quad G_\infty\right]^T$ of optimal model parameters. Guaranteed model approximation GMA [20,22] is adopted for the optimal choice of the best regularization parameter $\hat{\lambda}$. The numerical realization of the scheme by using the singular value decomposition (SVD [1]) is discussed and the resulting computer algorithm is also outlined in the previous paper [22]. The model $\overline{G}_K\left(t\right)$ of the relaxation modulus $\overline{G}(t)$ (2) is described by:

$$\overline{G}_K\left(t\right)=G_K\left(t\right)+G_\infty=\sum_{k=0}^{K-1} g_k\,\phi_k\left(t\right)+G_\infty, \tag{6}$$

where: the form of the functions $\phi_k(t)$ are given by Theorem 1 in the paper [22]. Theoretical and simulational analysis of the identification algorithm properties and the resulting optimal model is the purpose of this paper. The proofs of the main results are omitted due to space limitations. The applications example is also given.

IDENTIFICATION SCHEME

The calculation of the relaxation spectrum model involves the following steps:

1. Perform the stress relaxation test [18,19] and record the measurements $\overline{G}(t_i)$, $i=1,\ldots,N$, of the relaxation modulus at times $t_i \geq 0$.
2. Compute the matrix $\boldsymbol{\Phi}_{N,K}$ [22; eq. (16)] and next examine if $\boldsymbol{\Phi}_{N,K}{}^T\overline{\boldsymbol{G}}_N \neq \boldsymbol{0}_{K+1}$, where $\overline{\boldsymbol{G}}_N=\left[\overline{G}\left(t_1\right) \quad \ldots \quad \overline{G}\left(t_N\right)\right]^T$ is the vector of measurement data. If not, select new time-scale parameter α and/or a new number K of the basis functions and repeat Step 2 or repeat the experiment (Step 1). Otherwise go to Step 3.
3. Determine SVD decomposition of the matrix $\boldsymbol{\Phi}_{N,K}$:

$$\boldsymbol{\Phi}_{N,K}=\boldsymbol{U}\boldsymbol{\Sigma}\boldsymbol{V}^T, \tag{7}$$

   where: $\boldsymbol{\Sigma}=diag(\sigma_1,\ldots,\sigma_r,0,\ldots,0)$ is $N\times(K+1)$ diagonal matrix containing the non-zero singular values $\sigma_1,\ldots,\sigma_r$ of the matrix $\boldsymbol{\Phi}_{N,K}$ with $r=rank(\boldsymbol{\Phi}_{K,K})$ and $\boldsymbol{V}\in R^{K+1,K+1}$ and $\boldsymbol{U}\in R^{N,N}$ are orthogonal uniquely defined matrices [1].
4. Compute $Q_N\left(\overline{\boldsymbol{g}}_K^N\right)$ according to the formula $Q_N\left(\overline{\boldsymbol{g}}_K^N\right)=\sum_{i=r+1}^{N} y_i^2$, where y_i are the elements of the vector $\boldsymbol{Y}=\boldsymbol{U}^T\overline{\boldsymbol{G}}_N$ and $\overline{\boldsymbol{g}}_K^N$ is the normal solution of the original (not regularized) least-squares problem (5), (6) for noise data.
5. Chose $\hat{Q}_N > Q_N\left(\overline{\boldsymbol{g}}_K^N\right)$.
6. Solve the GMA equation:

$$\sum_{i=1}^{r}\frac{\lambda^2 y_i^2}{\left(\sigma_i^2+\lambda\right)^2}+Q_N\left(\overline{\boldsymbol{g}}_K^N\right)=\hat{Q}_N, \tag{8}$$

and compute the best regularization parameter $\hat{\lambda}$.

Compute the regularized solution:

$$\hat{\boldsymbol{g}}_K=\boldsymbol{g}_K^{\hat{\lambda}}=\boldsymbol{V}\Lambda_{\hat{\lambda}}\boldsymbol{U}^T\overline{\boldsymbol{G}}_N, \tag{9}$$

where: the diagonal structure matrix:

$$\Lambda_{\hat{\lambda}}=diag\left(\sigma_1\Big/\left(\sigma_1^2+\hat{\lambda}\right),\ldots,\sigma_r\Big/\left(\sigma_r^2+\hat{\lambda}\right),0,\ldots,0\right).$$

Determine the spectrum of relaxation frequencies $\hat{H}_K\left(\nu\right)$ according to (cf. (3)):

$$\hat{H}_K\left(\nu\right)=\sum_{k=0}^{K-1}\hat{g}_k\,h_k\left(\nu\right), \tag{10}$$

where: $\hat{g}_k$ are the elements of vector $\hat{\boldsymbol{g}}_K$.

Obviously, $\overline{H}_K\left(\nu\right)=\hat{H}_K\left(\nu\right)+G_\infty\delta\left(\nu\right)$ is the relaxation spectrum of the form [22; eq.(14)] corresponding to the optimal model of relaxation modulus of the form (6).

Remark 1. Only the SVD of the matrix $\boldsymbol{\Phi}_{N,K}$ (7) is space and time consuming task of the scheme. The SVD is accessible in the form of optimized numerical procedures in most commonly used contemporary computational packets.

Remark 2. It is easy to note that the matrix $\boldsymbol{\Phi}_{N,K}$ (see [22; eq. (16)]) depends on the choice of the basis functions, in particular on the scaling factor α selection, as well as on the measurement points $\{t_i\}$, however does not depend on the experiment results. Thus, when the identification scheme is applied for successive samples of the material, the SVD of $\boldsymbol{\Phi}_{N,K}$ in step 3 have not to be multiple repeated, while the same time instants $\{t_i\}$ and the same model parameters α and K are kept.

Remark 3. The Hermite functions $h_k(\nu)$ defined by the formula (4) can be determined using Hermite polynomials $P_k(x)$ [22; eqs. (3),(4)]. Polynomials $P_k(x)$ are accessible in some computational packets; they may be also computed according to definitional recursive formula.

Remark 4. By the optimal choice of the scaling factor α, the best fit of the model to the experimental data can be achieved. However, in practice a simple rough rule for choosing the scaling factor α, based on the comparison of a few first functions from the sequence $\{\phi_k(t)\}$ for different values of α with the experimentally obtained function $\overline{G}(t)$ is quite enough. In the same manner, the number K of the series (6) elements can be initially evaluated. Thus, the choice both of the number K as well as the parameter α must be done *a posteriori*, after the preliminary experiment data analysis.

ANALYSIS

SMOOTHNESS

Since the Hermite basis functions $h_k(\nu)$, k=0,1,…, form an orthonormal basis in the Hilbert space $L_2(-\infty,\infty)$

of real-valued square-integrable functions on the interval $(-\infty,\infty)$ [15], for an arbitrary $H_K(\nu)$ of the form (3) the following estimation is valid:

$$\|H_K\|_2^2 = \int_0^\infty H_K(\nu)^2\, d\nu \le$$
$$\le \int_{-\infty}^{\infty} H_K(\nu)^2\, d\nu = \sum_{k=0}^{K-1}\sum_{j=0}^{K-1} g_k g_j \int_{-\infty}^{\infty} h_k(\nu) h_j(\nu)\, d\nu,$$

and whence finally:

$$\|H_K\|_2^2 \le \sum_{k=0}^{K-1} g_k{}^2 = \|\boldsymbol{g}_K\|_2^2. \tag{11}$$

Here: $\|\cdot\|_2$ means the square norm both in the real Euclidean space as well as in $L_2(0,\infty)$. Therefore, the smoothness of the regularized solution $\hat{\boldsymbol{g}}_K$ (9) guarantees that the fluctuations of the respective relaxation spectrum $\hat{H}_K(\nu)$ (10) are bounded. The Hermite algorithm is in fact quasi-orthogonal identification scheme.

STABILIZATION

The purpose of the regularization relies on stabilization of the resulting model vector $\boldsymbol{g}_K^\lambda$. The effectiveness of this approach can be evaluated by the following relations, which follow for an arbitrary regularization parameter immediately from Proposition 2.2 in [21].

Proposition 1. *Let $K\ge1$, $r=rank(\boldsymbol{\Phi}_{N,K})$ and regularization parameter $\lambda>0$. For the regularized solution $\boldsymbol{g}_K^\lambda$* [22; eq. (20)] *the following equality and inequality hold:*

$$\left\|\boldsymbol{g}_K^\lambda\right\|_2^2 = \sum_{i=1}^{r} \frac{\sigma_i^2 y_i^2}{\left(\sigma_i^2+\lambda\right)^2} < \sum_{i=1}^{r} \frac{y_i^2}{\sigma_i^2} = \left\|\overline{\boldsymbol{g}}_K^N\right\|_2^2, \tag{12}$$

where: $\overline{\boldsymbol{g}}_K^N$ is the normal solution of the linear-quadratic problem (5),(6).

Therefore, by (12) the following rule holds: the greater the regularization parameter λ is, the fluctuations of the vector $\boldsymbol{g}_K^\lambda$ are highly bounded. Thus, the regularization parameter controls the smoothness of the regularized solution. Simultaneously, however, the best – in the GMA sense – parameter $\hat{\lambda}$ is monotonically increasing function of $\hat{Q}_N$. Thus, it is immediately evident that, the worse the relaxation modulus measurements approximation quality is, the regularized vector $\hat{\boldsymbol{g}}_K$ and, in view of (11), the computed spectrum $\hat{H}_K(\nu)$ are highly smoothed. The upper bounds of the vector $\hat{\boldsymbol{g}}_K$ and the norm of spectrum $\hat{H}_K(\nu)$ are established by our next result.

Proposition 2. *Let $K\ge1$, $N\ge K$ and $\hat{Q}_N > Q_N\left(\overline{\boldsymbol{g}}_K^N\right)$. Then, for the GMA regularized solution $\hat{\boldsymbol{g}}_K$* (9) *the following estimations hold:*

$$\left\|\hat{H}_K\right\|_2^2 \le \|\hat{\boldsymbol{g}}_K\|_2^2 \le \left(\sum_{i=1}^{r}\sigma_i^2 y_i^2\right)\left(\sum_{i=1}^{r} y_i^2/\sigma_i^4\right)\Big/\left(\hat{Q}_N - \sum_{i=r+1}^{N} y_i^2\right). \tag{13}$$

CONVERGENCE

Let us estimate the regularized vector $\hat{\boldsymbol{g}}_K$ error, which is measured by the norm $\left\|\hat{\boldsymbol{g}}_K - \boldsymbol{g}_K^N\right\|_2$, where $\boldsymbol{g}_K^N$ is the normal solution of the least-squares task (5),(6) for noise-free data. Obviously, relaxation spectrum $\hat{H}_K(\nu)$ (10) is only approximation of that spectrum, which can be obtained in the class of models (3) by direct minimization (without regularization) of the quadratic index (5) for noise-free measurements, i.e. the approximation of the function $H_K^N(\nu) = \sum_{k=0}^{K-1} g_k^N h_k(\nu)$, where $\boldsymbol{g}_K^N$ are the elements of vector $\boldsymbol{g}_K^N$. We have the following convergence result.

Proposition 3. *Let $K\ge1$, $N\ge K$ and $\hat{Q}_N > Q_N\left(\overline{\boldsymbol{g}}_K^N\right)$. Then, the following inequalities hold:*

$$\left\|\hat{H}_K - H_K^N\right\|_2 \le \left\|\hat{\boldsymbol{g}}_K - \boldsymbol{g}_K^N\right\|_2 \le \frac{1}{\sigma_r}\sqrt{\hat{Q}_N - Q_N\left(\overline{\boldsymbol{g}}_K^N\right)} + \frac{1}{\sigma_r}\|\boldsymbol{z}_N\|_2, \tag{14}$$

where: $\boldsymbol{z}_N=[z(t_1)\ \dots\ z(t_N)]^T$ is the measurement noises vector.

Therefore, the vector $\hat{\boldsymbol{g}}_K$ converges to the normal solution $\boldsymbol{g}_K^N$, and the spectrum $\hat{H}_K(\nu)$ tends to the 'normal' spectrum $H_K^N(\nu)$ in each point ν, at which they are both continuous, linearly with respect to the norm $\|\boldsymbol{z}N\|_2$, as $\hat{Q}_N \to Q_N\left(\overline{\boldsymbol{g}}_K^N\right)$ and $\|\boldsymbol{z}N\|_2 \to 0$, simultaneously.

Thus, the accuracy of the spectrum approximation depend both on the measurement noises and the assumed model quality as well as on the singular values of the matrix $\boldsymbol{\Phi}_{N,K}$, which, in turn, depend on the proper selection of the time-stale factor α of $h_k(\nu)$ (see Remark 4).

SIMULATION STUDIES OF NOISE ROBUSTNESS

We now present the results of the theoretical and numerical studies of the influence of the measurement noises on regularized solution. The experiment simulations are conducted using Gaussian relaxation spectrum. Such an example illustrates most of the works concerning relaxation or retardation spectrum identification, for example [4,23].

Example 1. Consider viscoelastic material whose relaxation spectrum is described by the Gauss distribution:

$$H(\nu) = \frac{1}{6\sqrt{2\pi}} e^{-(\nu-20)^2/72}. \tag{15}$$

The corresponding relaxation modulus is described by:

$$G(t) = \frac{1}{2} e^{-20t+18t^2}\, erfc\left(3\sqrt{2}t - 5\sqrt{2}/3\right), \tag{16}$$

where: $erfc(t)$ is defined by [22; eq. (11)].

The spectrum $H(\nu)$ (15) is given in Figure 3 (dashed line). In experiment the sampling instants

t_i was generated in the constant period in time interval $\mathsf{T}=[0;0,4]$ seconds selected on the basis of the relaxation modulus $G(t)$ (16) course in time. In order to study the influence of the noise variance σ^2 on the vector of model parameters measurement noises $\{z_i\}$ have been generated randomly with uniform distribution on the interval $[-h,h]$ for $h=0{,}0005;0{,}001;0{,}005;0{,}01$ and $N=100,500,1000,5000,10000$. $h=0{,}01$ is 1% of the maximum value of $G(t)$ and $h=0{,}0005$ is about 1% of the mean value of the modulus. Such measurement noises are even strongest than the true disturbances recorded for the biological materials (see [21, Chapter 5.5.4]). In the case of the sugar beet sample from example 3 below disturbances have not exceeded 0,8% of the maximum value of $G(t)$ and have not exceeded 0,7% of the mean value of the modulus. The experiment have been repeated $n=500$ times for every pair (N,σ^2) for $K=6$ and $K=8$.

The distance between $\hat{\boldsymbol{g}}_K$ and the regularized parameter for noise-free measurements:

$$\tilde{\boldsymbol{g}}_K = \boldsymbol{g}_K^{\tilde{\lambda}} = \boldsymbol{V}\boldsymbol{\Lambda}_{\tilde{\lambda}}\boldsymbol{U}^T\boldsymbol{G}_N, \tag{17}$$

has been estimated by normalized mean error defined for n element sample as:

$$ERR\left(N,K,\sigma^2\right) = \frac{1}{n}\sum_{j=1}^{n}\left\|\hat{\boldsymbol{g}}_{K,j} - \tilde{\boldsymbol{g}}_{K,j}\right\|_2 \Big/ \left\|\tilde{\boldsymbol{g}}_{K,j}\right\|_2, \tag{18}$$

where: $\hat{\boldsymbol{g}}_{K,j}$ denote the regularized model parameter $\hat{\boldsymbol{g}}_K$ for noise case and $\tilde{\boldsymbol{g}}_{K,j}$ is the regularized noise-free parameter determined for j–th experiment repetition for a given pair (N,K), $j=1,\ldots,n$. Since in the experiment the sampling period has been constant the vector $\tilde{\boldsymbol{g}}_{K,j}$ does not depend on j, i.e. $\tilde{\boldsymbol{g}}_{K,j}=\tilde{\boldsymbol{g}}_K$. Relationship of $ERR(N,K,\sigma^2)$ on N and σ^2 is depicted in Figures 1 and 2.

The ranges of variation of the index $ERR(N,K,\sigma^2)$ obtained in the simulation experiment are given in table 1. Time-scale factor $\alpha=0{,}06[s]$ was taken and kept valid in all the simulation experiments. Since the index $Q_N\left(\bar{\boldsymbol{g}}_K^N\right)\Big/N$ was included in the range from 3,0722E-6 (for small noises) to 2,578E-4 (for strong noises), the assumed value of model approximation index $\hat{Q}_N$ was taken such that $\hat{Q}_N/N$ vary in the range from 0,050 to 0,087, respectively, for small and strong noises. The index $ERR(N,K,\sigma^2)$ depends on the noise variance as well as on the matrix $\boldsymbol{\Phi}_{N,K}$ and on the assumed value of model approximation index $\hat{Q}_N$. The index $ERR(N,K,\sigma^2)$ does not depend essentially on the number of measurements but significantly depends on the intensity of noises. The algorithm ensures very good noise robustness for small and medium disturbances; the index $ERR(N,K,\sigma^2)$ does not exceed 1,5%. For large noises the index $ERR(N,K,\sigma^2)$ do not exceed 8%. The next two examples show how the scheme proposed can be used in the relaxation spectrum identification.

Table 1. The ranges of variation of the error index $ERR(N,K,\sigma^2)$ obtained in the simulation experiment

$ERR(N,K,\sigma^2)$	h=0,0005	h=0,001	h=0,005	h=0,01
K=6	0,0022÷0,0049	0,0044÷0,0096	0,0219÷0,036	0,0402÷0,0791
K=8	0,006÷0,0095	0,0097÷0,0157	0,0465÷0,0643	0,0537÷0,077

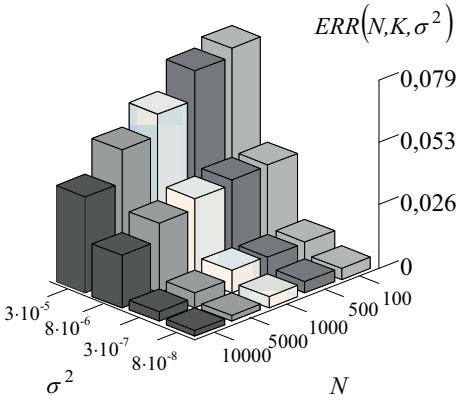

Fig. 1. The index $ERR(N,K,\sigma^2)$ as a function of N and σ^2 for $K=6$

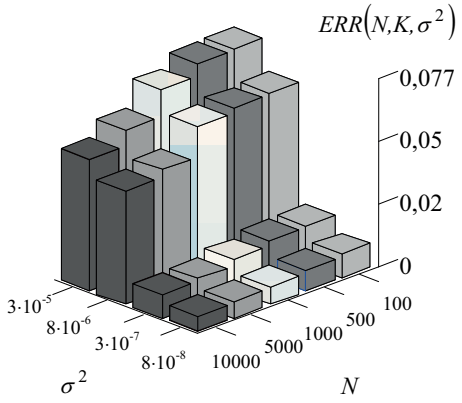

Fig. 2. The index $ERR(N,K,\sigma^2)$ as a function of N and σ^2 for $K=6$

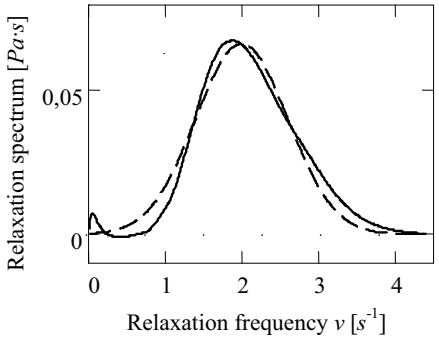

Fig. 3. Relaxation spectrum $H(\nu)$ (15) (dash line) and the approximated model $\hat{H}_K(\nu)$ (solid line).

Example 2. Let us consider again the Gaussian spectrum $H(\nu)$ (15). The modulus $\overline{G}(t) = G(t) + z(t)$ corrupted by noises $z(t)$ of the uniform distribution in the interval [–0,02; 0,2] has been sampled at $N=500$ instants at the constant period $\Delta t = 0{,}0008[s]$. The parameters $K=8$ and $\alpha = 0{,}06[s]$ are chosen according to Remark 4.

Since $Q_N\left(\overline{\boldsymbol{g}}_K^N\right) = 0{,}06495$, the assumed value of model quality is taken as follows: $\hat{Q}_N = 0{,}06527$. The GMA regularization parameter: $\hat{\lambda} = 5E\text{-}5$. The true relaxation spectrum $H(\nu)$ (15) and the resulting approximated model $\hat{H}_K(\nu)$ (10) are plotted in Figure 3.

RELAXATION SPECTRUM OF THE SUGAR BEET SAMPLE

Example 3. A cylindrical sample of 20 [*mm*] diameter and height was obtained from the root of sugar beet Janus variety [9]. During the stress relaxation test performed by Gołacki and co-workers [9], in the initial phase the strain was imposed instantaneously, the sample was preconditioned at the 0,5 [$m{\cdot}s^{-1}$] strain rate to the maximum strain. Next, during the second phase at constant strain the corresponding time-varying force induced in the specimen was recorded during the time period [0,5;96,2] seconds in 958 measurement points with the constant sampling period $\Delta t = 0{,}1[s]$. The experiment was performed in the state of uniaxial stress; i.e. the specimen examined underwent deformation between two parallel plates (for details see [9]). Modelling mechanical properties of this material in viscoelastic regime is justified in view of many studies, e.g., [2,9]. The respective relaxation modulus were computed using simple modification of the well-known Zapas and Craft rule [19] derived in [21].

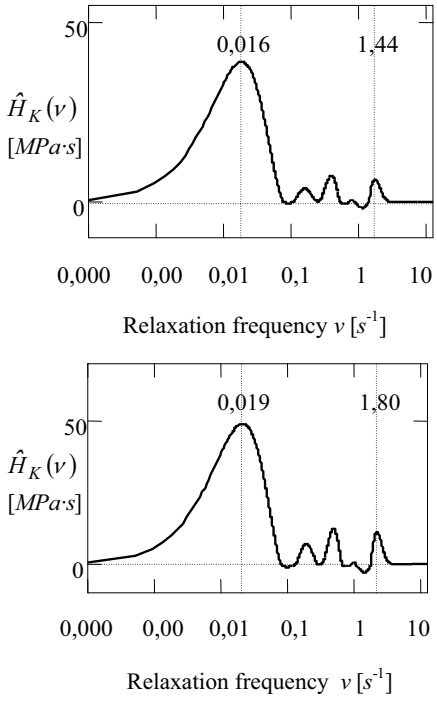

Fig. 4. The relaxation spectrum models $\hat{H}_K(\nu)$ of two samples of beet sugar root

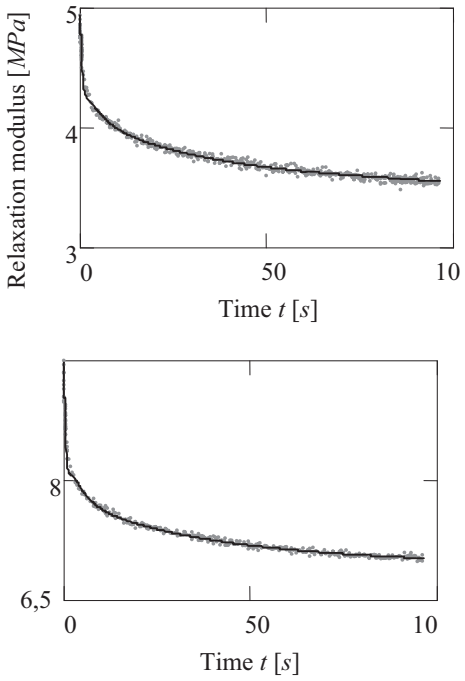

Fig. 5. The relaxation modulus measurements $\overline{G}(t_i)$ (points) and the best model $\overline{G}_K(t)$ (solid line) for two samples

The proposed identification scheme was applied and the relaxation spectra obtained are plotted in Figure 4 for two samples. The respective optimal models $\overline{G}_K(t) = \sum_{k=0}^{K-1} \hat{g}_k \phi_k(t) + \hat{G}_\infty$ are plotted in Figure 5, where the relaxation modulus measurements are also shown. For both samples $K=8$ and $\alpha = 10{,}4[s]$ was chosen. The computed long-term modulus was as follows: $\hat{G}_\infty = 3{,}436\,[MPa]$ and $\hat{G}_\infty = 6{,}877\,[MPa]$.

CONCLUSIONS

An algorithm has been found for the calculation of relaxation spectrum from the discrete-time measurement data of the linear relaxation modulus. Tikhonov regularization and guaranteed model approximation are used to solve it. As a result, the stability of the scheme is guaranteed. Due to the choice of the Hermite basis functions, for which the basis functions for relaxation modulus are given by the convenient recursive formula, the algorithm is very useful for implementation. This choice also guarantees that smoothing of the regularized solution ensures smoothing of the relaxation spectrum model. The choice of the scaling-time factor in order to achieve a good fit of the model to the experimental data is discussed and the noise robustness is demonstrated. It is also indicated that the accuracy of the spectrum approximation depends both on measurement noises and regularization parameter and on the proper selection of the time-scale parameter of the basis functions.

Although the paper is concerned with the relaxation spectrum identification using stress experiment data, a modification of the scheme proposed for determination of the retardation spectrum using the creep compliance

measurements obtained in creep test [18] is possible as well.

The proposed method \ provides us with the tool for relaxation spectrum identification applicable for an arbitrary viscoelastic material. We consider a situation where only the time-measurements from relaxation test are accessible for identification. This is important in studying the rheological properties of many materials, e.g., biodegradable materials [6], different pelets [3], livestock meat [17] and different plant materials [2, 9, 18]. The proposed method leads to insights into how to estimate the laws of such materials. Therefore it lies in the broad area of studying mechanical properties of such materials [7, 8, 10, 13,14].

REFERENCES

1. **Björck Å., 1996:** Numerical Methods for Least Squares Problems. SIAM, Philadelphia, PA.
2. **Bzowska-Bakalarz M., 1989:** Comparison of rheological models determining the physical properties of sugar beet roots. Proceedings of the 4th International Conference Physical Properties of Agricultural Materials, Rostock, 109-112.
3. **Czachor G., 2010:** Models of stress relaxation in fibreboards containing straw component. Inżynieria Rolnicza, 1(119), 105-113 [in Polish].
4. **Elster C., Honerkamp J., Weese J., 1991:** Using regularization methods for the determination of relaxation and retardation spectra of polymeric liquids. Rheological Acta 30(2), 161-174.
5. **Ferry J.D., 1980:** Viscoelastic properties of polymers. John Wiley and Sons, New York.
6. **Figiel A., 2008:** Rheological properties of biodegradable material determined on the basis of a cyclic stress relaxation test. Inżynieria Rolnicza, 4 (102), 271-278 [in Polish].
7. **Gładyszewska B., Ciupak A., 2011:** A storage time influence on mechanical parameters of tomato fruit skin. TEKA Commission of Motorization and Power Industry in Agriculture, 11C, 64-73.
8. **Gołacki K., Kołodziej P., 2011:** Impact testing of biological material on the example of apple tissue. TEKA Commission of Motorization and Power Industry in Agriculture, 11c, 74–82.
9. **Gołacki K., Kołodziej P., Stankiewicz A., Stropek Z., 2003:** Report of KBN Grant No 5P06F00619: "Mechanical hardiness of sugar beet analysis in the context of practical mechanical loads", 1-214 [in Polish].
10. **Guz T., 2008:** Thermal quarantine of apples as a factor forming its mechanical properties. TEKA Commission of Motorization and Power Industry in Agriculture, 8 A, 52-62.
11. **Honerkamp J., 1989:** Ill-posed problems in rheology. Rheological Acta, 28, 363–371.
12. **Kubacki K.S., 2006:** Should we always use the mean value. TEKA Commission of Motorization and Power Industry in Agriculture, 6, 55-66.
13. **Kuna-Broniowska I., Bożena Gładyszewska B., Anna Ciupak A., 2011:** A comparison of mechanical parameters of tomato's skin of greenhouse and soil-grown varieties. TEKA Commission of Motorization and Power Industry in Agriculture, 11C, 151-161.
14. **Kusińska E., Kornacki A., 2008:** Testing of a mathematical model of grain porosity. TEKA Commission of Motorization and Power Industry in Agriculture, 8A, 112-117.
15. **Lebedev N.N., 1972:** Special functions and their applications. Dover, New York.
16. **Ljung L., 1999:** System Identification: Theory for the User. Prentice-Hall, Englewood Cliffs New Jersey.
17. **Nowak K., Białobrzewski I., 2009:** Modelling rheological properties of livestock meat in Matlab environment. Inżynieria Rolnicza, 9(118), 177-180 [in Polish].
18. **Rao M.A., 1999:** Rheology of Fluid and Semisolid Foods. Principles and Applications. Aspen Publishers, Inc., Gaithersburg, Maryland.
19. **Sorvari J., Malinen M., 2006:** Determination of the relaxation modulus of a linearly viscoelastic material. Mechanics of Time-Dependent Materials, 10, 125–133.
20. **Stankiewicz A., 2003:** A scheme for identification of continuous relaxation time spectrum of biological viscoelastic materials. Acta Scientiarum Polonorum, Seria Technica Agraria 2(2), 77-91 [in Polish].
21. **Stankiewicz A., 2007:** Identification of the relaxation spectrum of viscoelastic plant materials. Ph. D. Thesis, Agricultural University of Lublin, Poland [in Polish].
22. **Stankiewicz A., 2012:** On determination of the relaxation spectrum of viscoelastic materials from discrete-time stress relaxation data. TEKA Commission of Motorization and Power Industry in Agriculture (submitted for publication).
23. **Syed Mustapha S.M.F.D., Phillips T.N., 2000:** A dynamic nonlinear regression method for the determination of the discrete relaxation spectrum. Journal of Physics D: Applied Physics, 33(10), 1219-1229.
24. **Tikhonov A.N., Arsenin V.Y., 1977:** Solutions of Ill-posed Problems. John Wiley and Sons New York, USA.

ALGORYTM IDENTYFIKACJI SPEKTRUM RELAKSACJI MATERIAŁÓW LEPKOSPRĘŻYSTYCH NA PODSTAWIE ZAKŁÓCONYCH POMIARÓW MODUŁU RELAKSACJI

Streszczenie. W pracy przedstawiono algorytm identyfikacji ciągłego spektrum relaksacji materiałów liniowo-lepkosprężystych na podstawie dyskretnych zakłóconych pomiarów z testu relaksacji naprężeń. Model spektrum relaksacji dany jest kombinacją liniową funkcji Hermita. Jego parametry dobrano optymalnie w sensie zregularyzowanej metody najmniejszej sumy kwadratów. Zastosowano regularyzację Tichonowa, współczynnik regularyzacji dobrano metoda gwarantowanej jakości modelu. Zbadano własności algorytmu i wyznaczonego modelu. Dla pomiarów z nałożonym szumem wykazano jego liniową zbieżność. Pokazano, że dokładność przybliżenia spectrum relaksacji zależy zarówno od intensywności zakłóceń oraz współczynnika regularyzacji jak i odpowiedniego doboru parametrów funkcji bazowych modelu. Przeprowadzone badania symulacyjne potwierdziły dokładność modelu i jego odporność na zakłócenia. Wyznaczono spektrum relaksacji dwu przykładowych próbek buraka cukrowego.

Słowa kluczowe: spektrum relaksacji, algorytm identyfikacji, regularyzacja, funkcje Hermita